# Safety-Metric Based Emergency Braking System Considering Both Lead and Following Vehicles in a Multi-Agent Environment

Sun-Yub, Park
Strategic Planning Division
Korea Intelligent Automotive Parts
Promotion Institute
Daegu, Korea
srad14@kiapi.or.kr

Yun-Ki, Yoon
Strategic Planning Division
Korea Intelligent Automotive Parts
Promotion Institute
Daegu, Korea
ykyoon@kiapi.or.kr

Kyung-Hwan, jeong
Strategic Planning Division
Korea Intelligent Automotive Parts
Promotion Institute
Daegu, Korea
kh.jeong@kiapi.or.kr

Bong-Seob, Kim
Strategic Planning Division
Korea Intelligent Automotive Parts
Promotion Institute
Daegu, Korea
bskim@kiapi.or.kr

Myung-Su, Lee
Strategic Planning Division
Korea Intelligent Automotive Parts
Promotion Institute
Daegu, Korea
trust@kiapi.or.kr

Kyung-Su, Yun
Strategic Planning Division
Korea Intelligent Automotive Parts
Promotion Institute
Daegu, Korea
kadbonow@kiapi.or.kr

Abstract— Over the past three decades, autonomous vehicles have expanded the Operational Design Domain (ODD) from highways to unstructured urban environments. In response, various technologies have been actively developed to ensure the safety of autonomous driving systems. However, the activation of Autonomous Emergency Braking (AEB) under hazardous conditions has introduced a new concern: the risk of secondary rear-end collisions. Despite this emerging issue, systematic strategies to mitigate such risks have not been sufficiently established. To address this issue, this study proposes a novel AEB system that integrates Responsibility-Sensitive Safety (RSS) with the Autonomous Driving Model (ADM). The autonomous vehicle collects real-time information on surrounding in-lane traffic through vehicle-to-infrastructure (V2I) communication and determines the AEB activation timing based on front and rear safety assessments using RSS and ADM. The proposed AEB framework effectively prevents or mitigates rear-end collisions typically induced by conventional AEB systems. Monte Carlo simulations, including case studies, were conducted to evaluate the performance of the proposed AEB system. Simulation results revealed a meaningful reduction in accident frequency and collision energy. This highlights the effectiveness of the proposed approach as a practical strategy for enhancing both safety and traffic flow, with expected contributions to the commercialization and further advancement of autonomous driving technologies.

Keywords—Autonomous driving, Autonomous Emergency Braking, Responsibility-Sensitive Safety, Autonomous Driving model, Vehicle-to-Infrastructure

## I. INTRODUCTION

According to the 2023 statistics from the Traffic Accident Analysis System (TAAS) of the Korea Road Traffic Authority, the total number of traffic accidents decreased by approximately 11.3%, from 223,552 cases in 2014 to 198,296 cases in 2023[1]. Among all reported cases, vehicle-to-vehicle collisions accounted for 152,935 cases (77.1%), with frontal collisions at 77,537 cases (50.7%) and rear-end collisions at 31,939 cases (20.9%), ranking first and second, respectively, among all accident types. In highway settings, 2,030 out of 5,220 accidents (38.9%) were rear-end collisions. According to the report "Final Rule: Automatic Emergency Braking Systems for Light Vehicles" (2024) published by the U.S. National Highway Traffic Safety Administration (NHTSA),

an analysis of data from 2010 to 2019 excluding 2020 and 2021 due to distortions caused by the COVID-19 showed that rear-end collisions were the most frequent type of crash, accounting for 32.5% of all traffic accidents. The number of rear-end collisions increased from 1,692 cases in 2010 to 2,363 cases in 2019. In addition, the proportion of fatal rear-end collisions rose from 5.6% in 2010 to 7.1% in 2019, marking a 1.5% increase over the period[2]. In response to the increasing prevalence of rear-end collisions, Euro NCAP began including the installation of AEB systems as an evaluation criterion in the safety assessment program in 2014 to encourage broader implementation. Nevertheless, the mitigation of rear-end collision risk remains insufficient[3].

The activation of an AEB system is classified as part of the mitigation phase according to international standards. During the mitigation process, vehicle environmental sensors monitor the lead vehicle and dynamic road environment in real time. When the real time evaluation of collision risk indicates that a predefined threshold has been exceeded, the system automatically activates emergency braking to either avoid the collision or mitigate the collision [4]. Various threat assessment methods have been proposed in the field of autonomous driving research to determine the activation timing of AEB systems. Time-To-Collision (TTC) is one of the most fundamental safety metrics, estimating the remaining time until a potential collision based on relative distance and velocity. Despite its simplicity, TTC does not consider relative acceleration or road surface conditions, limiting its applicability in dynamic driving environments. Time Headway (THW) is calculated by dividing the relative distance by the velocity of the ego vehicle. Although THW serves as an intuitive metric of traffic flow stability, the metric remains insensitive to critical situations because the value is unaffected even when the lead vehicle is at a complete stop. Deceleration Rate to Avoid a Crash (DRAC) calculates the equivalent deceleration required to avoid a collision and allows for direct comparison with the braking capability. However, the risk estimation based on DRAC may be underestimated, as the calculation does not reflect driver reaction delay or reduced road surface friction. Braking Threat Number (BTN) normalizes the DRAC by the maximum braking capability of the vehicle, enabling immediate identification of physically unavoidable collisions when the

value exceeds one. However, the metric is highly sensitive to estimation errors in braking performance and to variations in the road surface friction coefficient. The conventional RSS framework defines a minimum safe distance by incorporating multiple factors such as reaction delay and maximum deceleration, enabling the framework to serve as a foundation for legal reasoning. However, the formulation does not account for the safety margin of following vehicles[5], [6], [7], [8], [9], [10], [11]. Accordingly, recent reports have identified cases in which vehicles equipped with both Forward Collision Warning (FCW) and AEB systems exhibited approximately 20% higher rear-end collision rates compared to vehicles equipped with only FCW or low velocity AEB[12]. The observed increase in rear-end collision rates suggests that although AEB is effective in avoiding collisions with lead vehicles, the system remains insufficient in mitigating the risk of secondary rear-end collisions following abrupt deceleration. In addition, reliance on simple threshold based metrics such as TTC during mitigation scenarios likely contributes to the overestimation or underestimation of actual risk, as such metrics fail to adequately account for complex factors including changes in lead vehicle acceleration, variations in road surface friction, and the available response time of following vehicles. Therefore, minimizing accident damage requires the simultaneous consideration of both lead and following vehicles. In addition, a threat assessment and braking strategy based on comprehensive safety metrics, rather than simple threshold values, is essential for effective collision mitigation[13], [14], [15], [16].

To overcome the limitations of conventional RSS based models, this study proposes a following vehicle safety metric, termed RSS<sub>ADM</sub>, by extending the conventional RSS model to incorporate the unique characteristics of autonomous vehicles, including shorter reaction delays and enhanced braking and acceleration capabilities as well as an acceleration constraint that accounts for the safety margin of following vehicles. This approach enables precise assessment of both front and rear risks in multi-agent environments while maintaining rulebased safety guarantees. The ego vehicle receives real time information on surrounding in-lane traffic through V2I communication and evaluates the safety of both lead and following vehicles using RSS metrics. Once safety with respect to the lead vehicle is ensured, the ego vehicle assesses the predicted RSS<sub>ADM</sub> for the following vehicle to determine the appropriate activation timing of the AEB system.

The following are the contributions of this paper:

- RSS<sub>ADM</sub> is proposed as an extended following vehicle safety metric that integrates the ADM into the conventional RSS framework.
- An AEB system is proposed that determines the activation timing based on simultaneous safety evaluation of both lead and following vehicles using RSS and RSS<sub>ADM</sub>.

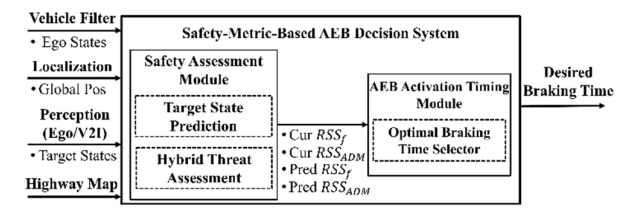


Fig. 1. Overall structure of the proposed algorithm.

#### II. OVERALL STRUCTURE OF THE PROPOSED ALGORITHM

The overall structure of the proposed algorithm is described in Fig. 1. The information required to perform the proposed algorithm is provided by the upper module, which consists of vehicle filtering, localization, and perception. Vehicle filtering identifies the ego vehicle's position, velocity, heading, and acceleration. Localization identifies the global position and route through map information, while perception recognizes the target vehicle's distance, velocity, and heading to the road through ego vehicle environment sensors and V2I perception and communication. The algorithm proposed in this study consists of two modules: The safety assessment module for lead and following vehicles evaluates safety conditions based on target vehicle information provided by the upper level module. The evaluation includes current RSS and current RSS<sub>ADM</sub>, as well as predicted front RSS and RSS<sub>ADM</sub> at each future time step. The AEB activation timing module determines the appropriate braking activation time based on the assessed safety metrics: namely, current RSS, current RSS<sub>ADM</sub>, predicted RSS, and predicted RSS<sub>ADM</sub>.

#### III. VEHICLE MODEL

The vehicle dynamics were modeled using a point-mass model, which simplifies the vehicle as a mass particle on a planar surface by neglecting complex body motions such as slip angle, pitch, and roll. The structure of the model is as follows:

$$\begin{aligned} x_{k+1} &= x_k + \cos(\theta_k) \cdot v_k \cdot dt \\ y_{k+1} &= y_k + \sin(\theta_k) \cdot v_k \cdot dt \\ \theta_{k+1} &= \theta_k + \gamma_k \cdot dt \\ v_{k+1} &= v_k + a_k \cdot dt \end{aligned} \tag{1}$$

The origin of the highway coordinate system is located at the center of the highway.  $x_k$ ,  $y_k$ ,  $\theta_k$  are the global x position, y position, and heading angle, based on the highway coordinate system. dt is the sampling time,  $v_k$  is the velocity,  $a_k$  is the acceleration, and  $\gamma_k$  is the yaw rate. Based on the highway map, a second-order polynomial regression equation is defined to connect the current location with the vehicle's driving route to a preview point with a preview time of 1.5 seconds:

$$y_{k} = ax^{2} + bx + c$$

$$\begin{bmatrix} y_{0} \\ y_{1} \\ y'(x_{0}) \end{bmatrix} = \begin{bmatrix} x_{0}^{2} & x_{0} & 1 \\ x_{1}^{2} & x_{1} & 1 \\ 2x_{0} & 1 & 0 \end{bmatrix} = \begin{bmatrix} a \\ b \\ c \end{bmatrix}$$
(2)

a, b, and c are coefficients used to define the curve from the current position to the target position. Given the driving route  $y_k$  defined by the 2nd-order polynomial regression equation, the curvature  $K_k$  is calculated using the first-order derivative and second-order derivative of the curve. The curvature  $K_k$  and the corresponding yaw rate  $Y_k$  are calculated as follows:

$$K_k = \frac{y''(x_0)}{\left\{1 + y'(x_0)^2\right\}^{\frac{3}{2}}} = \frac{2a}{\left\{1 + (2ax_0 + b)^2\right\}^{\frac{3}{2}}}$$
(3)

$$\gamma_k = v_{x,k} \cdot K_k \tag{4}$$

Based on the calculated yaw rate  $\gamma_k$ , the desired velocity and acceleration of the vehicle are calculated as follows:

$$v_{x,k} = \min\left(v_{x,des,max}, \max\left(v_{x,des,min}, \left|\frac{a_y}{\gamma_k}\right|\right)\right)$$
 (5)

$$a_{x,k} = \min \left( a_{x,max}, \max \left( a_{x,min}, \left( v_{x,cur} - v_{x,k} \right) \right) \right)$$
 (6)

 $v_{x,des,max}$ ,  $v_{x,des}$ , and minimum velocity values 16.7m/s and 1m/s, ay is a maximum lateral acceleration of 3m/s<sup>2</sup>. The desired velocity is adjusted according to minimum and maximum velocity constrained by lateral acceleration and yaw rate with vehicle dynamics and operating requirements. The  $v_{x,cur}$  and  $v_{x,k}$  represent the current velocity and the calculated desired velocity, respectively, while  $a_{x,k}$  represents the desired acceleration. The  $a_{x,k}$  value is adjusted according to the difference between the current state and the desired state so that the velocity is maintained within a specific range of highway traffic law constraints.

# IV. Brake Timing Determination Based on Safety Metrics

Heterogeneous autonomous vehicles, characterized by varying control software and driving policies, exhibit different levels of uncertainty across perception, decision making, and control domains. Therefore, the future trajectories of both lead and following vehicles are predicted simultaneously, and the activation timing of the AEB system is determined by applying integrated safety metrics such as stopping distance margin and reaction time margin. In this way, the proposed approach aims to prevent both underestimation and overestimation of actual risk, thereby enabling not only the avoidance of primary collisions with lead vehicles but also the mitigation of secondary rear-end collisions caused by sudden braking. Section A details the procedure for evaluating the safety of lead and following vehicles, while Section B describes the method for determining the AEB intervention timing based on the evaluation results.

#### A. Safety Assessment

This study confines the scope of risk analysis for collision avoidance and mitigation to the ego vehicle's lane (in-lane). On highways, steering based evasive maneuvers may trigger secondary collisions due to potential conflicts with adjacentlane vehicles or abrupt lateral movements by the ego vehicle. Therefore, the safety objective is focused on braking-based risk mitigation. The safety evaluation is structured in two stages. First, the future trajectories of both lead and following vehicles are predicted using a Kalman Filter (KF). Second, at each time step, RSS and RSS<sub>ADM</sub> are computed to account for the safety of the lead and following vehicles, respectively, and a composite risk index is derived by normalizing the relative distance based on both front and rear safety conditions. Each risk index is compared against a predefined threshold to classify the situation into either a safe range or a threat range. This section provides a detailed explanation of the calculation procedure and parameter setting methodology.

First, to predict the motion of both lead and following vehicles, the state transition model of the Extended Kalman Filter (EKF) is first defined. The inputs to the EKF consist of: (1) the driving path of surrounding vehicles included in the highway map, (2) target vehicle information received via V2I communication, and (3) surrounding vehicle information detected by the ego vehicle's environmental sensors. The nonlinear state transition function *f* is derived by substituting equations (4) and (6) into equation (1). Due to the nonlinearity

of the transition model, the process update is implemented in the form of an EKF. The prediction is based on the current information of surrounding vehicles, and considering that the driving scenarios do not involve significant environmental uncertainty, only the process update step is executed to ensure real time computational efficiency.

$$\mathbf{X}_k = [x_k \quad y_k \quad \theta_k \quad v_k]^T, \mathbf{u}_k = [\gamma_k \quad a_{x,k}]^T$$
 (7)

$$\widehat{\boldsymbol{X}}_{k+1} = f(\boldsymbol{X}_k, \boldsymbol{u}_k) = \begin{bmatrix} x_k + \cos(\theta_k) \cdot v_k \cdot dt \\ y_k + \sin(\theta_k) \cdot v_k \cdot dt \\ \theta_k + \gamma_k \cdot dt \\ v_k + a_k \cdot dt \end{bmatrix}$$
(8)

RSS defines the minimum longitudinal safe distance by assuming a worst case scenario. If the lead vehicle decelerates immediately at a rate no greater than the maximum deceleration, and the following vehicle accelerates during the reaction delay at a rate less than the maximum acceleration, then decelerates at least at the minimum deceleration until coming to a complete stop, a collision between the two vehicles does not occur. The basic RSS model defined in [15] is as follows:

$$d_{min} = \begin{bmatrix} v_r \rho + \frac{1}{2} a_{max,accel} \rho^2 + \frac{v_r^2}{2a_{min,brake}} \\ -\frac{v_f^2}{2a_{max,brake}} \end{bmatrix}_+$$
(9)

 $d_{min}$  represents the minimum longitudinal safe distance that the following vehicle must maintain from the lead vehicle to avoid a collision.  $v_r$  is the current velocity of the following vehicle, and  $\rho$  is the reaction delay of the following vehicle.  $a_{max,accel}$  represents the maximum acceleration the following vehicle may apply during the reaction delay, while  $a_{min,brake}$  represents the minimum guaranteed deceleration applied after the reaction period.  $v_f$  is the velocity of the lead vehicle, and  $a_{max,brake}$  represents the maximum deceleration the lead vehicle may apply immediately.

The basic RSS formulation guarantees a safe distance only with respect to the lead vehicle when the ego vehicle is positioned between leading and following vehicles, but it does not account for the rear safety margin required for the following vehicle to stop safely. To address this limitation, this study integrates the constant velocity travel distance and uniformly accelerated braking distance formulas, and introduces an ADM by replacing the human driver reaction delay specified in UNECE R157 with the response delay characteristic of autonomous systems[18]. From the perspective of the following vehicle, the ego vehicle acting as the lead vehicle limits its maximum deceleration  $a_{max.brake}$ to the value permitted by the ADM. In this way, the model ensures that the following vehicle can maintain the minimum longitudinal safe distance required to come to a complete stop without a collision. The ADM is defined as follows:

$$a_{ego,max}^{ADM} = \frac{v_{rel}^2}{2(d_{rear} - v_{rel}\rho)} + a_{TED}$$
 (10)

 $v_{rel}$  is the relative velocity with the following vehicle,  $d_{rear}$  is the relative distance,  $\rho$  is the reaction delay of the ego vehicle (set to 0.2 s), and  $a_{TED}$  represents the minimum guaranteed expected deceleration capability of the following vehicle, assumed to be 4m/s².

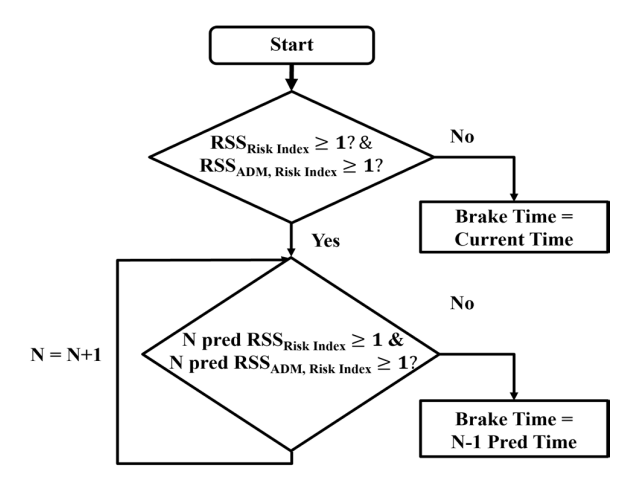


Fig. 2. Optimal AEB Activation Timing Selector

The final formulation of the minimum longitudinal safe distance with the following vehicle, as proposed in this study and represented as RSS<sub>ADM</sub>, is defined as follows:

$$d_{min,rear} = \begin{bmatrix} v_r \rho + \frac{1}{2} a_{max,accel} \rho^2 + \frac{v_r^2}{2 a_{min,brake}} \\ -\frac{v_f^2}{2 a_{ego,max}^{ADM}} \end{bmatrix}_{+}$$
(11)

The parameters used in the RSS model are set as follows:  $\rho=0.2s$ ,  $a_{max,accel}=1.5m/s^2$ ,  $a_{min,brake}=-4m/s^2$ , and  $a_{max,brake}=-6.64m/s^2$ . The parameters used in the RSS<sub>ADM</sub> model are set as follows:  $\rho=0.2s$ ,  $a_{max,accel}=1.5m/s^2$ ,  $a_{min,brake}=-4m/s^2$ , and  $a_{max,brake}=a_{ego,max}^{ADM}=ADM$  value.

## B. Optimal AEB Activation Timing Selector

This section describes the algorithm for determining the latest possible yet safe activation timing of the AEB system, based on the front and rear risk indices derived in Section A. The foremost principle of the algorithm is to ensure safety with respect to the lead vehicle at all times. Since rear safety cannot be considered unless front safety is first secured, the RSS condition must always be satisfied as the primary constraint, regardless of the situation. The algorithm decision flow of the Optimal AEB Activation Timing Selector is illustrated in Fig. 2.

## V. RESULTS

# A. Simulation Setting

This study assumes a four-lane bidirectional highway in Fig. 3 where collision and rear-end accidents frequently occur. The thick solid lines on the outer edges represent road shoulders, while the orange solid line in the center denotes bidirectional separation. From the infrastructure perspective, a Cooperative Intelligent Transport Systems(C-ITS) center and Road Side Units(RSUs) are installed along the roadway. RSU collects the position, driving direction, and velocity of each vehicles from vehicle V2I communication packets, and transmits this information to the C-ITS center. The center is assumed to integrate and process the collected data and redistribute it to nearby vehicles via the RSUs in the form of V2I messages. Fig. 3 visualizes the overall traffic scenario in a global coordinate system centered on the midpoint of the highway.

TABLE I. INITIAL CONDITION FOR CASE STUDY

| Vehicle | D <sub>DTO,ini</sub> (m) | V <sub>ini</sub> (m/s) | V <sub>max</sub> (m/s) |
|---------|--------------------------|------------------------|------------------------|
| Ego     | 117                      | 8.3                    | 16.7                   |
| Target1 | 82                       | 6.9                    | 13.9                   |
| Target2 | 102                      | 8.3                    | 16.7                   |
| Target3 | 157                      | 8.3                    | 19.4                   |
| Target4 | 67                       | 6.9                    | 16.7                   |

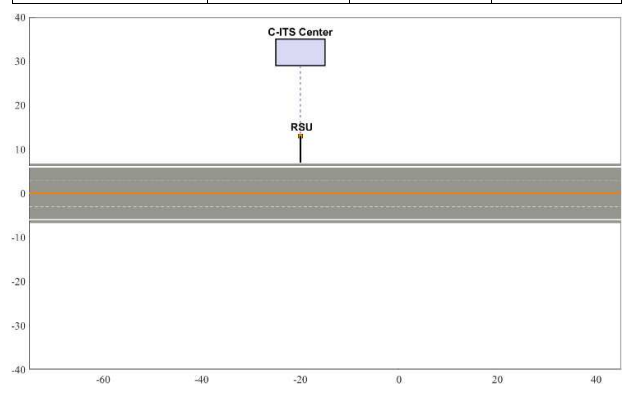


Fig. 3. Highway Simulation Map with C-ITS Center and RSU.

#### B. Case Study

Fig. 4 is the simulation scenario for the case study. A driving situation is assumed in which one ego vehicle and six target vehicles are traveling together on a highway. Among them, two target vehicles are already stopped on the road due to a prior collision. Target 1, which is the lead vehicle of the ego vehicle, is configured in a scenario where it detects a hazard and activates emergency braking immediately after a cut-out event occurs, in which the preceding vehicle departs from the lane to avoid the collision site.

The ego vehicle follows Target 1 while maintaining ACC level 1(i.e., a 15m following distance at a velocity of 15m/s). When Target 1 performs emergency braking to avoid the accident, the ego vehicle classifies the situation as a mitigation phase and proceeds to evaluate the safety conditions of both the lead and following vehicles. Based on the results of this evaluation, the AEB activation timing is determined once, and no further reassessment is performed thereafter.

Fig. 5 shows the minimum safe distances for both lead and following vehicles, as well as the actual relative distances, calculated at each time step from the moment the ego vehicle enters the mitigation phase until it comes to a complete stop.

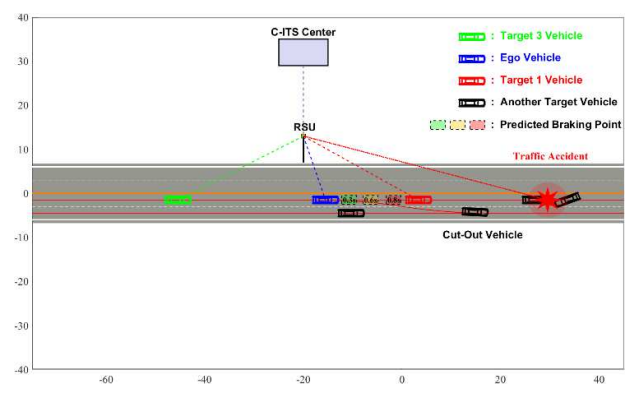


Fig. 4. Highway Case Study Simulation Scene.

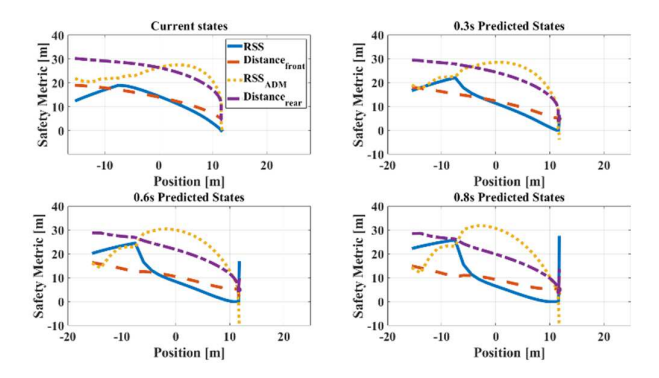


Fig. 5. Safety-Metric Results for the Case Study.

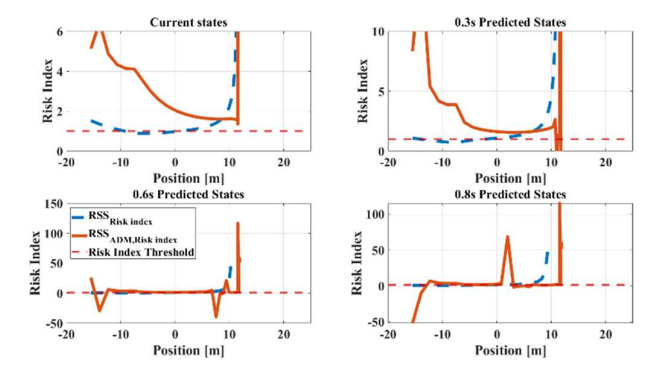


Fig. 6. Risk-Index Results for the Case Study

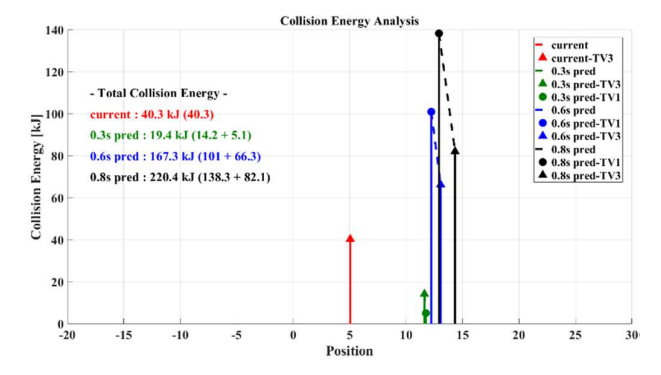


Fig. 7. Per-Time Step Collision Results for Vaildating the Risk-Index Based AEB Activation Timing for the Case Study.

Fig. 6 shows the time-varying risk indices calculated by normalizing the front and rear relative distances obtained from Fig. 5 with their respective RSS values. As described earlier in Chapter 4, Section A, the algorithm first satisfies the RSS condition as the primary constraint before considering the RSS<sub>ADM</sub>. The graphs, arranged in top-left, top-right, bottomleft, and bottom-right order, respectively display the RSS Risk Index and RSS<sub>ADM</sub> Risk Index at the current time, and at predicted time steps of 0.3s, 0.6s, and 0.8s. A Risk Index of 1 or greater indicates a safe range, and the horizontal Risk Index Threshold line represents the safety compliance boundary. At the current time step and the 0.3s prediction step, both the RSS Risk Index and the RSS<sub>ADM</sub> Risk Index satisfy their respective safety threshold values. At the 0.6s prediction step, only the RSS<sub>ADM</sub> Risk Index satisfied the safety threshold, whereas the RSS Risk Index did not. At the 0.8s prediction step, neither index satisfied the threshold. Therefore, the Optimal AEB Activation Timing Selector determined the 0.3s prediction step among the time steps where both the front and rear Risk

Index values simultaneously meet the safety threshold as the activation time for AEB, allowing the greatest safety margin for the following vehicle.

Fig. 7 shows the collision energy results from simulations in which AEB was activated at each time step, in order to verify the validity of AEB activation timing based on the RSS Risk Index and RSS<sub>ADM</sub> Risk Index. TV1 refers to the lead vehicle Target 1, and TV3 refers to the following vehicle Target 3. At the current time step, AEB is triggered immediately upon entering the mitigation phase without considering rear-end risk. While the early AEB activation successfully avoids a front collision, it results in a rear-end collision with TV3, generating a collision energy of 40.3kJ. on the other hand, when AEB was activated at the 0.3s prediction step as determined by the proposed algorithm, lead vehicle safety was ensured while also accounting for the safety of the following vehicle. As a result, a collision with TV3 occurred with an collision energy of 14.2kJ, followed by a secondary collision of 5.1kJ, resulting in a total collision energy of 19.4kJ. When AEB was activated at the later prediction steps of 0.6s and 0.8s, the delayed braking led to severe collisions of 167.3kJ and 220.4kJ, respectively. As a result, the proposed safety-metric based Optimal AEB Activation Timing Selector reduced the collision energy by approximately 51.9% compared to the immediate braking approach, demonstrating a significant reduction in accident severity under the same conditions.

#### C. Monte-Carlo Simulation

To analyze the performance under various scenarios, a Monte Carlo simulation approach was employed. A total of 100 simulations were conducted, with each simulation using randomly generated initial conditions as specified in Table 2.

Fig. 8 presents the results of the Monte Carlo simulation, showing the collision rates of the proposed algorithm and the conventional approach. The proposed algorithm achieved a collision rate of 0.61, which represents a 7.58% reduction compared to the conventional method's rate of 0.66. The black error bars on the bars indicate the 95% confidence interval. Due to the high variance in the experimental data, the  $3\sigma$  interval was found to be excessively wide and was thus replaced with the 95% confidence interval.

Fig. 9 shows the average and maximum collision energies from 100 Monte Carlo simulations. The proposed algorithm reduced the average collision energy to 152.8kJ, compared to 198.2kJ for the conventional method, a 22.93% reduction. Proposed algorithm also reduced the maximum (peak) collision energy to 230.1kJ from 267.8kJ, achieving a 14.09% decrease. These results demonstrate that optimizing AEB activation timing based on front and rear risk indices can significantly reduce accident severity.

TABLE II. INITIAL CONDITION FOR MONTE-CARLO

| Vehicle | $D_{DTO,ini}(m)$ | V <sub>ini</sub> (m/s) | V <sub>max</sub> (m/s) |
|---------|------------------|------------------------|------------------------|
| Ego     | N(120, 20)       | N(8.3, 1.4)            | N(16.7, 1.4)           |
| Target1 | N(80, 20)        | N(6.9, 1.4)            | N(13.9, 1.4)           |
| Target2 | N(100, 20)       | N(8.3, 1.4)            | N(16.7, 1.4)           |
| Target3 | N(160, 20)       | N(8.3, 1.4)            | N(19.4, 1.4)           |
| Target4 | N(70, 20)        | N(6.9, 1.4)            | N(16.7, 1.4)           |

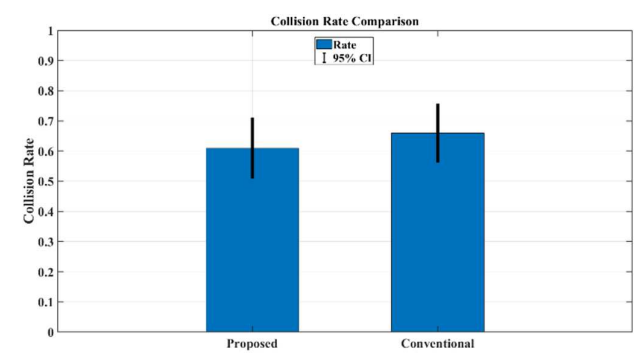


Fig. 8. Collision Rate (100 MC, 95% CI) : Proposed vs Conventional.

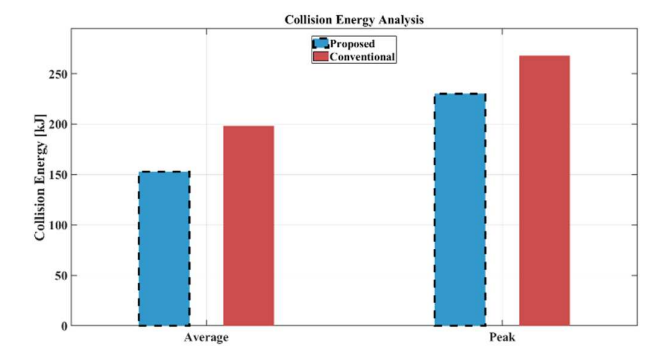


Fig. 9. Collision Energy (100 MC): Proposed vs Conventional.

#### VI. CONCLUSION

This study proposes a safety-metric based AEB system that considers both lead and following vehicles, aiming to minimize rear-end collision risks of autonomous vehicles in a multi-agent traffic environment comprising heterogeneous agents characterized by varying control software and driving policies. By integrating the rule-based RSS with the ADM an adaptation of the HDM that reflects the performance characteristics of autonomous vehicles the proposed system preserves rule-based safety guarantees while enabling simultaneous and precise assessment of front and rear risks in multi agent traffic environments. The case study and Monte Carlo simulation results demonstrate that the proposed Risk-Index based Optimal AEB Activation Timing Selector accurately evaluates both front and rear risks to determine the optimal activation timing, significantly reducing collision rates and collision energy by up to 51.9% across the case study and 100 Monte Carlo trials. This demonstrates the proposed algorithm's effectiveness in improving core autonomous driving safety functions and reducing accident damage. In future work, the scope of scenarios will be expanded to include steering based evasive maneuvers, in order to validate the applicability of the proposed risk index. In addition, the applicability of the proposed system to real world driving will be comprehensively evaluated through Hardware-in-the-Loop (HIL) testing.

#### ACKNOWLEDGMENT

This work was supported by Institute of Information & communications Technology Planning & Evaluation (IITP)

grant funded by the Korea government (MSIT) (No.2021-0-

01415, Development of multi-agent simulation & test scenario generation SW for edge connected autonomous driving service verification).

#### REFERENCE

- KoROAD, "Traffic Accident Statistics 2024 Edition (2023 Statistics)," Republic of Korea, 2024.
- [2] NHTSA, "Federal Motor Vehicle Safety Standards; Automatic Emergency Braking Systems for Light Vehicles," U.S. Dept. Transp., Final Rule, Docket No. NHTSA-2023-0021, RIN 2127-AM37, 49 CFR Parts 571, 595, and 596, Washington, DC, USA, 2024.
- [3] Euro NCAP, "Autonomous Emergency Braking (AEB) Car-to-Car," Euro NCAP, [Online]. Available: 2014.
- [4] UNECE, "UN Regulation No. 152–Uniform provisions concerning the approval of motor vehicles with regard to the Advanced Emergency Braking System (AEBS) for M1 and N1 vehicles," E/ECE/TRANS/505/Rev.3/Add.151, Geneva, Switzerland, Oct. 30, 2020
- [5] A. A. Sharizli, R. Rahizar, M. R. Karim, and A. A. Saifizul, "New Method for Distance-based Close Following Safety Indicator". Traffic Injury Prevention, vol. 16, no. 1, pp. 190–195, 2014.
- [6] A. Doi, T. Butsuen, T. Niibe, T. Takagi, Y. Yamamoto, and H. Seni, "Development of a rear-end collision avoidance system with automatic brake control," Jsae Rev., vol. 15, no. 4, pp. 335–340, 1994.
- [7] J. Jansson, "Collision avoidance theory: With application to automotive collision mitigation," Ph.D. dissertation, Linköping Univ. Electron. Press, Linköping, Sweden, 2005.
- [8] H. Singh, B. Weng, S. J. Rao, and D. Elsasser, "A diversity analysis of safety metrics comparing vehicle performance in the lead-vehicle interaction regime," 2023, arXiv:2306.14657.
- [9] Y. Lin and M. Althoff, "CommonRoad-CriMe: A toolbox for criticality measures of autonomous vehicles," in *Proc. IEEE Intell.* Veh. Symp., 2023, pp. 1–8.
- [10] S. Shalev-Shwartz, S. Shammah, and A. Shashua, "On a formal model of safe and scalable self-driving cars," 2017, arXiv:1708.06374. [Online]. Available: http://arxiv.org/abs/1708.06374
- [11] S. Rajendar and V. K. Kaliappan, "Recent advancements in autonomous emergency braking: A survey," in *Proc. 5th Int. Conf. Electron.*, Commun. Aerosp. Technol., 2021, pp. 1027–1032.
- [12] J. B. Cicchino, "Effectiveness of forward collision warning and autonomous emergency braking systems in reducing front-to-rear crash rates," *Accident Anal. Prevention*, vol. 99, pp. 142–152, Feb. 2017, doi: 10.1016/j.aap.2016.11.009.
- [13] C. Wang, C. Popp, and H. Winner, "Acceleration-based collision criticality metric for holistic online safety assessment in automated driving," *IEEE Access*, vol. 10, pp. 70662–70674, 2022.
- [14] D. Åsljung, J. Nilsson, and J. Fredriksson, "Comparing collision threat measures for verification of autonomous vehicles using extreme value theory," *IFAC-PapersOnLine*, vol. 49, no. 15, pp. 57–62, 2016. [Online].
- [15] Y. Zhang, E. Antonsson, and K. Grote, "A new threat assessment measure for collision avoidance systems," in Proc. IEEE Intell. Transp. Syst. Conf., 2006, pp. 968–975.
- [16] P. Koopman, B. Osyk, and J. Weast, Autonomous Vehicles Meet the Physical World: RSS, Variability, Uncertainty, and Proving Safety. Cham, Switzerland: Springer, 2019.
- [17] A. Andersson, "Multi-target threat assessment for autonomous emergency braking," M.S. thesis, Chalmers University of Technology, 2016. [Online].
- [18] UNECE, "UN Regulation No. 157–Uniform provisions concerning the approval of vehicles with regard to Automated Lane Keeping Systems (ALKS)," E/ECE/TRANS/505/Rev.3/Add.156, Geneva, Switzerland, 2021